JPEDAV (2007) 28:250–257
DOI: 10.1007/s11669-007-9085-y
1547-7037 ©ASM International

Thermodynamic Modeling of the Ag-Au-Sb Ternary System

E. Zoro, C. Servant and B. Legendre

(Submitted March 14, 2006)

A thermodynamic assessment of the Ag-Au-Sb ternary system has been carried out using the CALPHAD method based on new thermodynamic and phase equilibria data that we have recently determined. The Ag-Sb binary system has also been reoptimized. The calculated phase diagram and thermodynamic properties of the ternary system Ag-Au-Sb show satisfactory general agreement with the experimental data. The liquidus projection and monovariant valleys of the ternary system are well reproduced by the optimized thermodynamic model parameters. Additional experiments to confirm the proposed reaction scheme, which involves two ternary transition peritectic reactions, are suggested.

Keywords Ag-Au-Sb (silver-gold-antimony) system, Calphad method, COST 531, optimization, phase diagram, solder, thermodynamics

1. Introduction

Due to environmental and health concerns, a substantial amount of research is currently being carried out to develop new solder alloys capable of replacing the traditional lead-based solder alloys.[1] To design suitable lead-free substitute solders, it is necessary to evaluate several properties of the various candidate alloy systems. The properties required to be known include the phase diagram and thermodynamic properties since these provide basic information on the phase stability of each phase involved in a stable or metastable equilibria, liquidus and solidus temperatures, phase compositions and phase fractions at any given alloy composition and temperature. In addition, the thermodynamic approach will help to understand and predict the various possible interfacial reactions between the solder and the substrate materials. Therefore, a detailed knowledge of the thermodynamic properties and phase equilibria for these alloy systems obtained via critical thermodynamic evaluations based on sound thermodynamic models is an essential first step in the successful design of new solder alloy systems.

The components of the Ag-Au-Sb ternary system are among the selected elements defined by the COST 531 (COopération Scientifique et Technique)[2] program as lead-free solder candidates. The only previous experimental study of the Ag-Au-Sb ternary system is that published by Burkhard et al.[3] These authors showed that the (ε) Ag_3Sb phase extends into the Ag-Au-Sb system as a single phase up to about 10 at.% Au. In our more recent paper,[4] the Ag-Au-Sb phase diagram was studied experimentally using x-ray diffraction (XRD) analysis, electron-probe micro-analysis (EPMA), and differential scanning calorimetry (DSC). In addition, the enthalpies of mixing of the liquid alloys in the Ag-Au-Sb system were determined using Tian-Calvet Calorimetry.[5] In this paper we present the results of a thermodynamic assessment of the Ag-Au-Sb ternary system carried out using the CALPHAD method. Calculated results obtained with the optimized dataset are compared with the original experimental data points.

E. Zoro and **C. Servant,** Laboratoire de Physico-Chimie de l'Etat Solide, ICMMO, UMR 8182, Bât 410-415, Orsay Cedex 91405, France; **E. Zoro** and **B. Legendre,** Laboratoire de Chimie Physique Minérale et Bioinorganique, EA401, Fac. Pharm., Université de Paris-Sud XI, 5, rue JB Clément, Châtenay Malabry 92296, France; Contact e-mail: colette.servant@lpces.u-psud.fr

2. Data Used for the Thermodynamic Assessment

2.1 Phase Diagram Data

The following binary system assessments were chosen: Ag-Au from Hassam et al.,[6] Au-Sb by Kim et al.[7] As for the Ag-Sb binary system, we have re-assessed this from the work of Oh et al.,[8] in order to get better agreement between the calculated $(L+\zeta)/L$ and $(L+\varepsilon)/L$ phase boundaries, (Fig. 1), and our experimental data. The calculated liquid compositions obtained for the peritectic reaction at 829.5 K and the eutectic reaction are compromise values between those of Okamoto[9] and Oh[8], (Table 1).

As no previous experimental study exists for the Ag-Au-Sb ternary system, we first determined experimentally[4] the phase equilibria occurring in this system. In particular, the temperatures of the liquidus and invariant reactions were measured for four vertical sections (80, 70, 10 at.% Ag, and 10 at.% Au). As no ternary compound was found,[4] the rule of Rhines[10] allows us to state that three invariant reaction planes exist in this system. The three-phase domains have the hcp_A3 (ζ) ternary phase in common. In fact, the hcp_A3 (ζ) of the Ag-Sb binary system phase extends into

the ternary system by dissolution of about 40 at.% Au. The experimental isothermal section at 613 K studied by EPMA enabled the triangulation of the ternary system. The three-phase domains are: $\zeta + (Sb) + \varepsilon$, $\zeta + (Sb) + AuSb_2$ and $\zeta + AuSb_2 + \alpha$. All of these data were used in optimizing the thermodynamic parameters for the different phases present in the Ag-Au-Sb system.

2.2 Thermodynamic Data

Among the enthalpies of mixing data of the liquid alloys, previously determined experimentally[5] for the eight sections at different temperatures shown in Fig. 2, only those measured on seven sections were used to assess the thermodynamic parameters of the liquid phase: Au:Sb = 3:7 at 834 K, Au:Sb = 1:4 at 833 K, Au:Sb = 2:3 at 743 K, Ag:Sb = 3:7 at 834 K, Ag:Sb = 7:3 at 873 K, Ag:Sb = 3:7 and 1:4 at 873 K. The initial values are from the optimized binary systems Au-Sb[7] and Ag-Sb.[11] The data from the section Au:Sb = 1:4 at 873 K, which differed too much for two runs, were discarded during the optimization procedure.

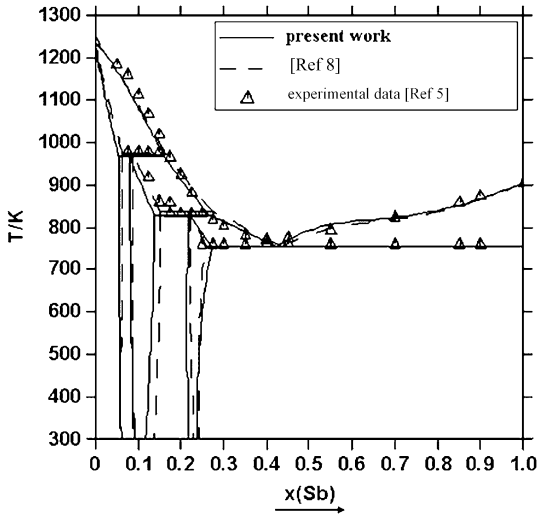

Fig. 1 Comparison between the present re-assessed Ag-Sb phase diagram and that of Oh[8] plus our experimental points[4]

3. Thermodynamic Modeling

The Ag-Au-Sb system exhibits five substitutional solution phases, fcc (α), hcp (ζ), orthorhombic (ε), rhombohedral (Sb) and liquid, and one intermediate stoichiometric compound ($AuSb_2$).

The molar Gibbs energies of the substitutional solution phases (ϕ) were expressed as follows:

$$G_m^{\phi} = x_{Ag}{}^0G_{Ag} + x_{Au}{}^0G_{Au} + x_{Sb}{}^0G_{Sb} + RT(x_{Ag}\ln x_{Ag} + x_{Au}\ln x_{Au} + x_{Sb}\ln x_{Sb}) + {}^{ex.}G_m^{\phi} \quad \text{(Eq 1)}$$

where

$${}^{ex.}G_m^{\phi} = x_{Ag}x_{Au}L_{Ag,Au}^{\phi} + x_{Ag}x_{Sb}L_{Ag,Sb}^{\phi} + x_{Au}x_{Sb}L_{Au,Sb}^{\phi} + x_{Ag}x_{Au}x_{Sb}L_{Ag,Au,Sb}^{\phi} \quad \text{(Eq 2)}$$

${}^0G_i$ and x_i denote the Gibbs energy and site or mole fraction of the component i, respectively. $L_{i,j}^{\phi}$ and $L_{i,j,k}^{\phi}$, which are expressed by the Redlich-Kister-Muggianu[12,13] polynomial, are the interaction energy between the elements i and j and ternary interaction parameter, respectively. $L_{i,j}^{\phi}$ and $L_{i,j,k}^{\phi}$, can be dependent on both composition and temperature.

Optimization of the Gibbs energy parameters of the phases was carried out by the Calphad method[14] using the PARROT module of the ThermoCalc software.[15] The pure solid elements at 25 °C (298.15 K) in their stable forms were chosen as the reference state of the system. The Scientific Group Thermodata Europe (SGTE) unary data published by Dinsdale[16] were used for the thermodynamic functions of the pure elements in their stable and metastable states.

The substitutional solution phases in the binary and ternary systems were modeled as follows:

- one sublattice for the liquid phase :$(Ag,Au)_1$:, :$(Ag,Sb)_1$:, :$(Au,Sb)_1$:, :$(Ag,Au,Sb)_1$:,

Table 1 Invariant equilibria occurring in the Ag-Sb binary system: comparison between our calculated values and results from Oh et al.[8] and Okamoto[9]

	Present work		[8]		[9]	
Invariant reactions	***T*, K**	***x*, at.% Sb**	***T*, K**	***x*, at.% Sb**	***T*, K**	***x*, at.% Sb**
$L + \alpha \leftrightarrow \zeta$	967.7	$x_{Sb}^{L} = 16.08$	974.5	$x_{Sb}^{L} = 16.32$	975.7	$x_{Sb}^{L} = 16.9$
		$x_{Sb}^{\alpha} = 5.43$		$x_{Sb}^{\alpha} = 6.36$		$x_{Sb}^{\alpha} = 7.2$
		$x_{Sb}^{\zeta} = 8.00$		$x_{Sb}^{\zeta} = 8.79$		$x_{Sb}^{\zeta} = 8.5$
$L + \zeta \leftrightarrow \varepsilon$	829.5	$x_{Sb}^{L} = 26.51$	835.6	$x_{Sb}^{L} = 27.67$	835.2	$x_{Sb}^{L} = 25.0$
		$x_{Sb}^{\zeta} = 13.81$		$x_{Sb}^{\zeta} = 15.27$		$x_{Sb}^{\zeta} = 16.4$
		$x_{Sb}^{\varepsilon} = 21.67$		$x_{Sb}^{\varepsilon} = 22.01$		$x_{Sb}^{\varepsilon} = 21.1$
$L \leftrightarrow \varepsilon + (Sb)$	755.8	$x_{Sb}^{L} = 42.31$	753.2	$x_{Sb}^{L} = 43.61$	758.2	$x_{Sb}^{L} = 41.0$
		$x_{Sb}^{\varepsilon} = 27.17$		$x_{Sb}^{\varepsilon} = 25.57$		$x_{Sb}^{\varepsilon} = 25.0$
		$x_{Sb}^{(Sb)} = 100$		$x_{Sb}^{(Sb)} = 100$		$x_{Sb}^{(Sb)} = 100$

- one sublattice for the rhombohedral phase :$(Sb)_1$:,
- two sublattices for the Fcc_A1 phase :$(Ag,Au)_1$:$(Va)_1$:, :$(Ag,Sb)_1$:$(Va)_1$:,:$(Au,Sb)_1$:$(Va)_1$:, :$(Ag,Au,Sb)_1$:$(Va)_1$:, (Va for Vacancy);
- two sublattices for the Hcp_A3 phase :$(Ag,Au)_1$:$(Va)_{0.5}$:,: $(Ag,Sb)_1$:$(Va)_{0.5}$:, :$(Au,Sb)_1$:$(Va)_{0.5}$:,:$(Ag,Au,Sb)_1$:$(Va)_{0.5}$:,
- two sublattices for the orthorhombic Ag_3Sb (ε-phase :$(Ag,Sb)_{0.75}$: $(Ag,Sb)_{0.25}$:, :$(Ag,Au,Sb)_{0.75}$: $(Ag,Au,Sb)_{0.25}$:, and the Wagner-Schottky model[17] of additivity of energy in the sublattices was used.
- two sublattices for the $AuSb_2$ compound :$(Ag)_{0.33333}$: $(Sb)_{0.66667}$:, :$(Ag,Au)_{0.33333}$:$(Sb)_{0.66667}$:.

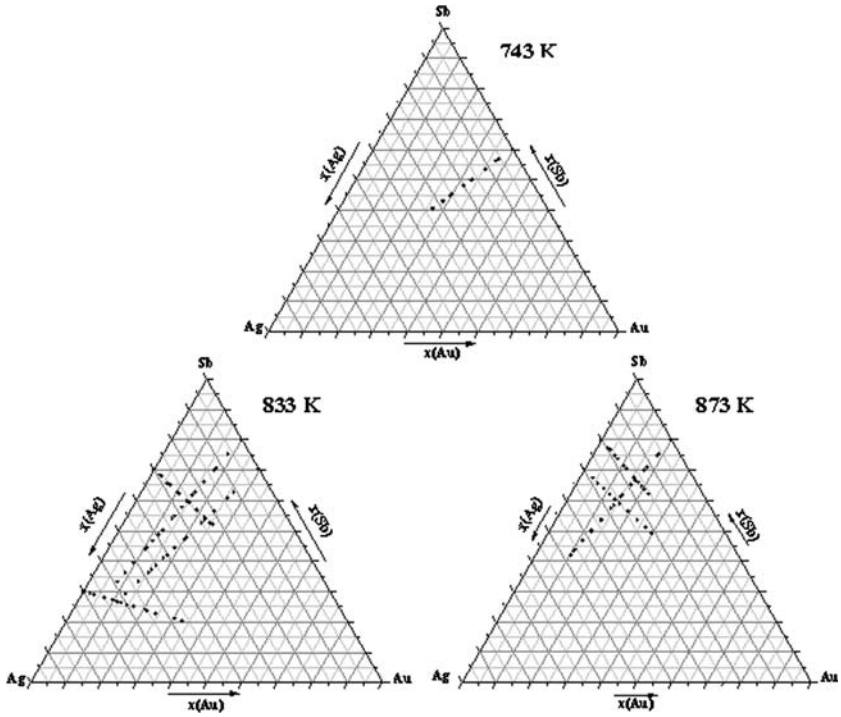

Fig. 2 Composition sections and temperatures used in the calorimetric determinations of the enthalpies of mixing of Ag-Au-Sb liquid alloys[4]

Table 2 Comparison of experimental and calculated invariant reactions occurring in the Ag-Au-Sb system (with a = 2641.1228 J/mol)

	Reaction type		Temperature, K			Compositions, at.%	
						Au	Sb
Invariant reactions	Calc.	Exp.	Calc.	Exp.	Phase	Calc.	
$L + \varepsilon \leftrightarrow \zeta + (Sb)$	U	U_1	688.1	690.0	L	15.44	38.53
					ε	9.52	25.17
					ζ	14.19	17.50
					(Sb)	0	100
$L + (Sb) \leftrightarrow \zeta + AuSb_2$	E_1	U_2	661.8	662.0	L	25.04	39.43
$L \leftrightarrow (Sb) + \zeta + AuSb_2$[a]					ζ	24.12	15.79
					(Sb)	0	100
					$AuSb_2$	31.17	66.67
$L + \zeta \leftrightarrow \alpha + AuSb_2$	E_2	U_3	663.1	650.0	L	38.74	36.34
$L \leftrightarrow AuSb_2 + \zeta + \alpha$[a]					ζ	40.68	10.57
					α	56.69	0.29
					$AuSb_2$	32.84	66.67

[a]Calculation results

Table 3 The thermodynamic properties of the Ag-Au-Sb ternary system (the unit is J/mol)

Elements

(298.13<T<3000.00)

Ag in AGSB_ORTHO (ε)

${}^{0}G_{\mathrm{Ag:Ag}}^{\mathrm{AGSB\_ORTHO}} - {}^{0}H_{\mathrm{Ag}}^{\mathrm{SER}} = +5000 + \mathrm{GHSERAG}.$

Au in AGSB_ORTHO (ε)

${}^{0}G_{\mathrm{Au:Au}}^{\mathrm{AGSB\_ORTHO}} - {}^{0}H_{\mathrm{Au}}^{\mathrm{SER}} = +5000 + \mathrm{GHSERAU}.$

Sb in AGSB_ORTHO (ε)

${}^{0}G_{\mathrm{Sb:Sb}}^{\mathrm{AGSB\_ORTHO}} - {}^{0}H_{\mathrm{Sb}}^{\mathrm{SER}} = +5000 + \mathrm{GHSERSB}.$

Systems

Ag-Au

(298.13 < T < 3000.00)

Liquid

${}^{0}L_{\mathrm{Ag,Au}}^{\mathrm{liquide}} = -16402 + 1.14 \times T.$

(298.13 < T < 3000.00)

Fcc (α)

${}^{0}L_{\mathrm{Ag,Au:VA}}^{\mathrm{fcc}} = -15599.00$

(298.13 < T < 3000.00)

Hcp (ζ)

${}^{0}L_{\mathrm{Ag,Au:VA}}^{\mathrm{hcp}} = -15599.$

AGSB_ORTHO (ε)

${}^{0}G_{\mathrm{Ag:Au}}^{\mathrm{AGSB\_ORTHO}} - 0.75 \times {}^{0}H_{\mathrm{Ag}}^{\mathrm{SER}} - 0.25 \times {}^{0}H_{\mathrm{Au}}^{\mathrm{SER}} = +0.75 * \mathrm{GHSERAG} + 0.25 * \mathrm{GHSERAU}.$

${}^{0}G_{\mathrm{Au:Ag}}^{\mathrm{AGSB\_ORTHO}} - 0.75 \times {}^{0}H_{\mathrm{Au}}^{\mathrm{SER}} - 0.25 \times {}^{0}H_{\mathrm{Ag}}^{\mathrm{SER}} = +10000 + 0.75 \times \mathrm{GHSERAU} + 0.25 \times \mathrm{GHSERAG}\ .$

Ag-Sb

(298.13 < T < 3000.00)

Liquid

$L_{\mathrm{Ag,Sb}}^{\mathrm{liquide}} = -964.4779 - 7.9876 \times T + (-21481.357 + 7.1738 \times T)(x_{\mathrm{Ag}} - x_{\mathrm{Sb}}) - 9992.0766 \times (x_{\mathrm{Ag}} - x_{\mathrm{Sb}})^2.$

Fcc (α)

$L_{\mathrm{Ag,Sb:VA}}^{\mathrm{fcc}} = -30164.027 + 66.4033 \times T + (+8714.5741 - 67.6783 \times T)(x_{\mathrm{Ag}} - x_{\mathrm{Sb}}).$

Hcp (ζ)

$L_{\mathrm{Ag,Sb:VA}}^{\mathrm{hcp}} = -24173.95 + 44.2101 \times T + (-2341.9664 - 49.1982 \times T)(x_{\mathrm{Ag}} - x_{\mathrm{Sb}}).$

(298.13 < T < 3000.00)

AGSB_ORTHO (ε)

${}^{0}G_{\mathrm{Ag:Sb}}^{\mathrm{AGSB\_ORTHO}} - 0.75 \times {}^{0}H_{\mathrm{Ag}}^{\mathrm{SER}} - 0.25 \times {}^{0}H_{\mathrm{Sb}}^{\mathrm{SER}} = +0.75 \times \mathrm{GHSERAG} + 0.25 \times \mathrm{GHSERSB} - 411.8398 - 3.8229 \times T.$

${}^{0}G_{\mathrm{Sb:Ag}}^{\mathrm{AGSB\_ORTHO}} - 0.75 \times {}^{0}H_{\mathrm{Sb}}^{\mathrm{SER}} - 0.25 \times {}^{0}H_{\mathrm{Ag}}^{\mathrm{SER}} = +0.75 \times \mathrm{GHSERSB} + 0.25 \times \mathrm{GHSERAG} + 10000 + 411.8398 + 3.8229 \times T$

${}^{0}L_{\mathrm{Ag:Ag,Sb}}^{\mathrm{AGSB\_ORTHO}} = -5788.5398.$

${}^{0}L_{\mathrm{Ag,Sb:Sb}}^{\mathrm{AGSB\_ORTHO}} = 10491.79.$

Au-Sb

(298.13 < T < 3000.00)

Liquid

$L_{\mathrm{Au,Sb}}^{\mathrm{liquid}} = -10288.0428 - 14.7865028 \times T + (-2901.66787 - 7.2503632 \times T)(x_{\mathrm{Au}} - x_{\mathrm{Sb}}) + (+1217.43604 - 4.74909763 \times T)(x_{\mathrm{Au}} - x_{\mathrm{Sb}})^2.$

Fcc (α)

${}^{0}L_{\mathrm{Au,Sb:VA}}^{\mathrm{fcc}} = +31456.5511 - 35.1097911 \times T$

(298.13 < T < 1000.00)

Hcp (ζ)

${}^{0}L_{\mathrm{Au,Sb:VA}}^{\mathrm{hcp}} = 7580.$

(298.14 < T < 2000.00)

Au-Sb_2

${}^{0}G_{\mathrm{Ag:Sb}}^{\mathrm{AuSb_2}} - 0.333333 \times {}^{0}H_{\mathrm{Ag}}^{\mathrm{SER}} - 0.666667 \times {}^{0}H_{\mathrm{Sb}}^{\mathrm{SER}} = +0.333333 \times \mathrm{GHSERAG} + 0.666667 \times \mathrm{GHSERSB} + 2641.12288.$

${}^{0}G_{\mathrm{Au:Sb}}^{\mathrm{AuSb_2}} - 0.333333 \times {}^{0}H_{\mathrm{Au}}^{\mathrm{SER}} - 0.666667 \times {}^{0}H_{\mathrm{Sb}}^{\mathrm{SER}}$
$= +0.333333 \times \mathrm{GHSERAU} + 0.666667 \times \mathrm{GHSERSB} - 5721.66949 + 6.93505837 \times T - 0.62 \times T \times LN(T).$

(298.13 < T < 3000.00)

AGSB_ORTHO (ε)

${}^{0}G_{\mathrm{Sb:Au}}^{\mathrm{AGSB\_ORTHO}} - 0.75 \times {}^{0}H_{\mathrm{Sb}}^{\mathrm{SER}} - 0.25 \times {}^{0}H_{\mathrm{Au}}^{\mathrm{SER}} = +10000 + 0.75 \times \mathrm{GHSERSB} + 0.25 \times \mathrm{GHSERAU}.$

${}^{0}G_{\mathrm{Au:Sb}}^{\mathrm{AGSB\_ORTHO}} - 0.75 \times {}^{0}H_{\mathrm{Au}}^{\mathrm{SER}} - 0.25 \times {}^{0}H_{\mathrm{Sb}}^{\mathrm{SER}} = +0.75 \times \mathrm{GHSERAU} + 0.25 \times \mathrm{GHSERSB}.$

Table 3 continued

Elements
Ag-Au-Sb
(298.13 < T < 3000.00)
Liquid
$L^{\text{liquid}}_{\text{Ag,Au,Sb}} = (-70007.00 + 10.002 \times T)x_{\text{Ag}} + (14955.98 - 6.5513 \times T)x_{\text{Au}} + (10.00 - 30.00 \times T)x_{\text{Sb}}$.
Fcc (α)
$L^{\text{fcc}}_{\text{Ag,Au,Sb:VA}} = (-40000.00 + 13.30 \times T)x_{\text{Ag}} + (102555.776 - 0.3686 \times T)x_{\text{Au}} + (-681.4882 - 0.9398 \times T)x_{\text{Sb}}$.
Hcp (ζ)
$L^{\text{hcp}}_{\text{Ag,Au,Sb:VA}} = (-124000.00 + 34.00 \times T)x_{\text{Ag}} + (3000.00 + 0.6248 \times T)x_{\text{Au}} + (4000.00 + 10^{-3} \times T)x_{\text{Sb}}$.
(298.13 < T < 3000.00)
AGSB_ORTHO (ε)
${}^0L^{\text{AGSB\_ORTHO}}_{\text{Ag,Au:Sb}} = -11750.00 + 9.15 \times T$.
${}^0L^{\text{AGSB\_ORTHO}}_{\text{Ag:Ag,Au,Sb}} = -48000.00$.
${}^0L^{\text{AGSB\_ORTHO}}_{\text{Ag,Au:Ag,Sb}} = -35500.00 + 9.8585 \times T$

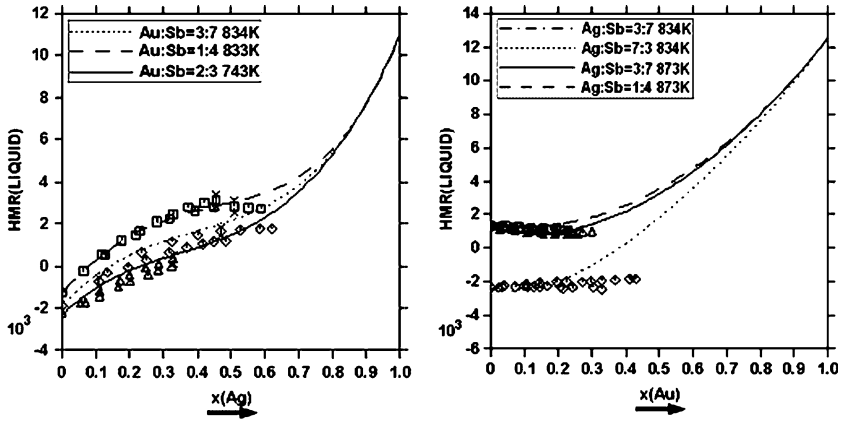

Fig. 3 Calculated enthalpies of mixing (in J/mol) of the Ag-Au-Sb liquid phase for seven isoplethal sections at the temperatures indicated. The symbols give our calorimetric values[4] and the curves the present calculations. For the calculations, all phases other than the liquid are suspended

4. Results and Discussion

The complete thermodynamic dataset for the Ag-Au-Sb system is given in Table 3. This comprises the data for the pure components, the edge binary systems and the optimized ternary parameters for the liquid, fcc, hcp and ε-phases. In Fig. 3, the calculated enthalpies of mixing for the Ag-Au-Sb liquid phase are compared with the calorimetric data points in plots of $\Delta_{\text{mix}}H^{\text{L}}$ vs. composition at three different fixed Au:Sb ratios and four fixed Ag:Sb ratios. Overall the agreement between the calculated and experimental values is good. The apparent discrepancy between the experimental and calculated values for the Au:Sb = 1:4 section compositions higher than x(Ag) = 0.5 is due to precipitation of the ζ phase in the calorimetric measurements whereas for the calculations all phases except the liquid phases are suspended. In addition, the section Ag:Sb = 3:7 shows that a difference of 39 K has no effect on the enthalpy of mixing values (Fig. 3b, where the curves noted as – and - - - are superimposed).

Further comparisons between calculated results and experiment are made in Fig. 4 which shows four calculated vertical sections at 70 at.% Ag, 10 at.% Au, 10 at.% Ag, and 10 at.% Ag in the Sb-rich region. It can be seen that the agreement between the calculated boundaries and the experimental results is generally good. However, with the 70 at.% Ag section (Fig. 4a) discrepancies exist between calculation and experiment for both the $L/(L + \alpha)$ liquidus and the $(L + \zeta)/\zeta$ solidus curves. The same situation arises with the $(L + \zeta)/(L + \zeta + \varepsilon)$ phase boundary on the 10 at.% Au section (Fig. 4b). This fact may be due to the lack of sufficient experimental data for the ζ phase.

The 10 at.% Ag section (Fig. 4c, d) reveals a difference with the interpretation of our experimental results. In fact, in contrast to our conclusions listed in Table 2 (three transition peritectic reactions (labeled as U_1, U_2 and U_3), were determined through calculation, two eutectic reactions (labeled as E_1 and E_2) and one transition peritectic reaction (noted U). The calculated U_3 reaction (E_2) occurs at a temperature (663.1 K) slightly higher (1.3 K) than the

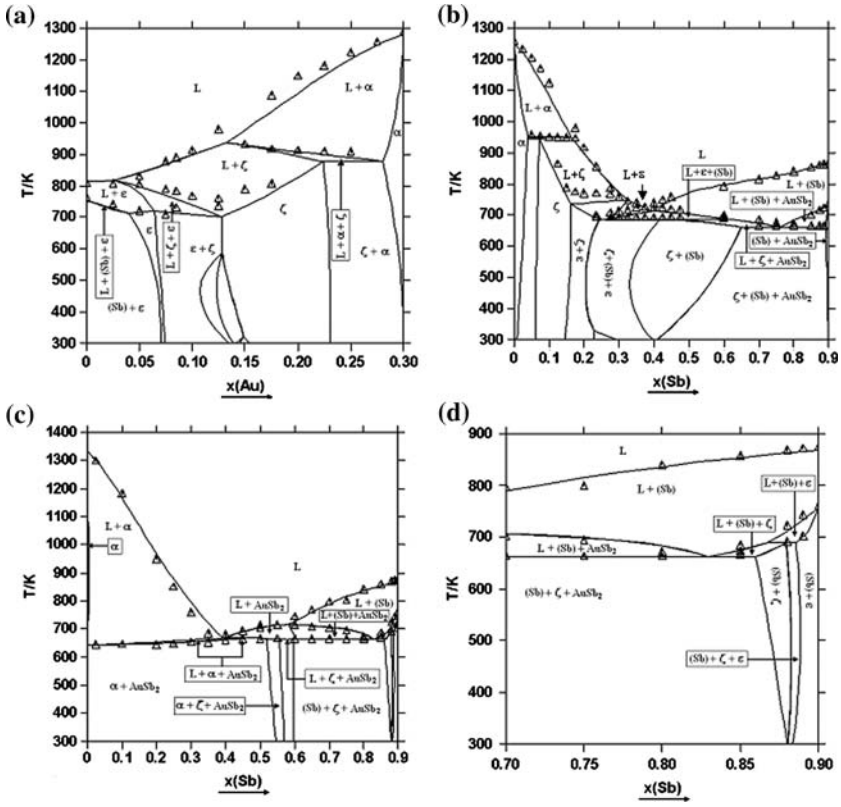

Fig. 4 Calculated vertical sections through the Ag-Au-Sb phase diagram plus our experimental points;[4] (a) 70 at.% Ag section, (b) 10 at.% Au section, (c) 10 at.% Ag section, (d) 10 at.% Ag section in the Sb-rich region

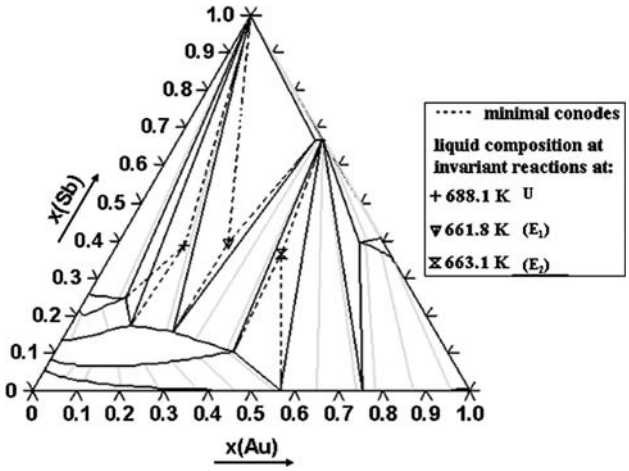

Fig. 5 Calculated Ag-Au-Sb isothermal section at 661.8 K with one U-type and two E-type reactions superimposed

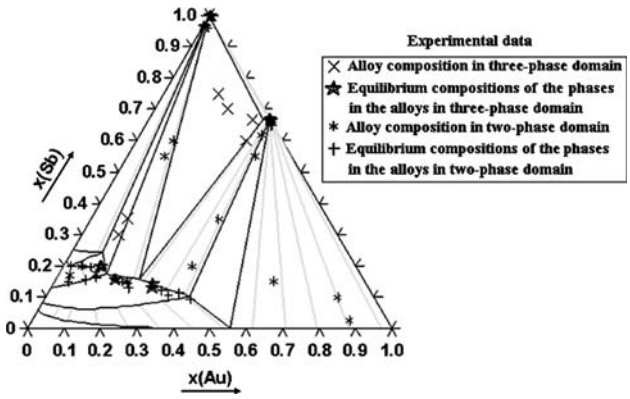

Fig. 6 Calculated Ag-Au-Sb isothermal section at 613 K with experimental data superimposed

calculated U_2 reaction (E_1) at 661.8 K. It will be noted in Fig. 7,[4] on the 10 at.% Au vertical section, that the temperatures of the invariant reactions U_1 and U_2 are determined on a larger composition range than the U_3 reaction. In fact, the U_3 reaction is materialized by only two data points: 0.35 at. Sb (649.9 K) and 0.40 at. Sb (650.0 K), which have been determined on the experimental 10 at.% Ag vertical section shown in Fig. 6.[4] Experimentally, the temperatures are theoretically determined with an accuracy of ±5 K for the thermal treatments and ±0.5 K for the DSC measurements. But in fact, as a function of the position of the samples in the furnace of thermal treatment or in the DSC device and/or of the existence of a very small amount of impurities in the samples, such temperature discrepancies can exist and may change our reaction scheme. During our optimization procedure, the statistical

weighting given to the data points of the U_3 invariant reaction were lower than those of the U_2 and U_1 reactions. A slight change in the value of the optimized enthalpy term (noted as *a*) of the thermodynamic parameter *G*:Ag:Sb: of the phase (Ag,Au)Sb_2 (a decrease from 2641.1228 (see Table 3) to 1400 J/mol) moves the order of occurrence of the U_2 (E_1) and U_3 (E_2) reactions, respectively, at 663.7 and 663.6 K. However, a small maximum of temperature then exists on the valleys: e_2 (630.7 K)-*max. (664.3 K)*-E_2 (663.1 K) and E_1 (661.8 K)-*max. (667.9 K)*-E_2 (663.1 K) and both reactions remain eutectic. The change in *a* causes only a very slight extension of the (Ag,Au)Sb_2 phase on the isothermal ternary section calculated at 613 K. When the change in *a* is somewhat larger (*a* = 150 J/mol), U_2 occurs at 668.3 K and U_3 at 664.7 K. No maximum is noted on the E_1-E_2 monovariant valley and the U_2 (E_1) invariant reaction is therefore peritectic. But the U_3 (E_2) reaction remains eutectic because a small maximum (at 668.6 K) is observed on the E_2-e_2 valley. For this latter value of the *a* parameter, the extension of (Ag,Au)Sb_2 on the isothermal ternary section stays reasonable but somewhat more important than the experimental one. So, further experimental determinations are therefore necessary to affirm that the U_3 reaction really occurs at 650 K and to clarify the exact reaction scheme for U_2 and U_3. In Fig. 5, these calculated invariant reactions are shown on an isothermal section calculated at 661.8 K, as well as the composition of the liquid phase. It will be noted that for the calculated *U* (experimental U_1) peritectic reaction, the composition of the liquid phase is, as it has to be, outside of the triangle drawn from the calculated chemical compositions of the three solid phases (ε-ζ-(Sb)) whilst for the two calculated eutectic reactions, the composition of the liquid phase is in fact inside the invariant triangles ((Sb)-ζ-$AuSb_2$) and ($AuSb_2$-ζ-α). It is not far from the outside of the triangles and at the limit of one side ($AuSb_2$-ζ) of each triangle. These two transition "peritectic" reactions may be degenerate.

On the other hand, Fig. 6 shows the ternary isothermal section at 613 K. Good agreement with the experimental

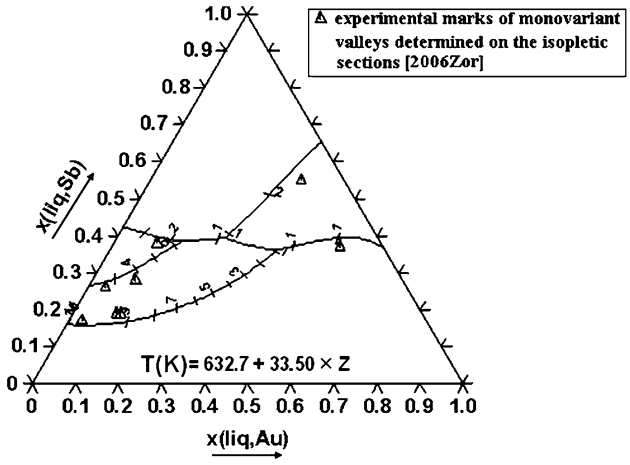

Fig. 7 Calculated projection of the monovariant valleys present in the liquidus surface

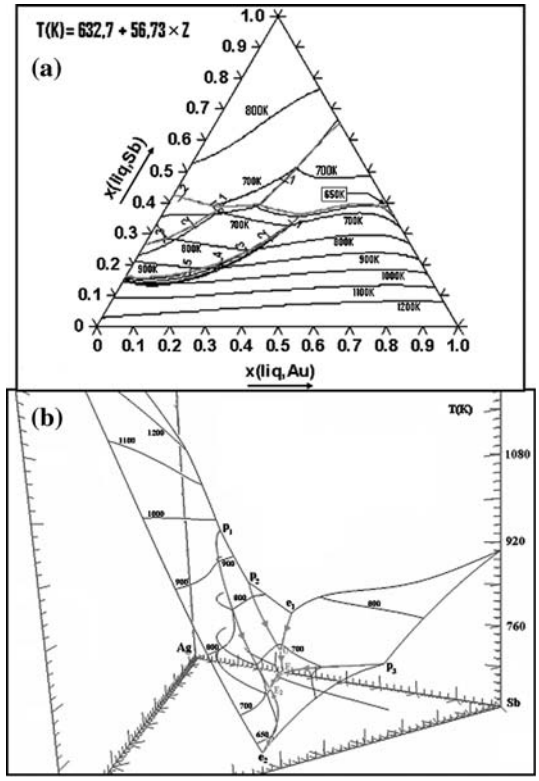

Fig. 8 Calculated liquidus surface isotherms and monovariant valleys of the Ag-Au-Sb ternary system. (a) Projection in the Gibbs triangle. The numbers from 1 to 5 give the values taken by *z* in the equation for the temperature in Kelvin. (b) Three-dimensional view

results is noted. However, the ε and ζ alloy compositions of the alloys in the respective $\varepsilon + \zeta + (Sb)$ and $\zeta + AuSb_2 + (Sb)$ three-phase triangles are slightly different from the experimental measurements (Fig. 6, see the stars corresponding to the equilibrium compositions of the phases of the alloys in the three-phase domains).

The calculated liquidus projection for the Ag-Au-Sb system, given in Fig. 7, is in good agreement with the experimental data for the compositions (noted as Δ of the monovariant valleys. We also calculated the isotherms of the liquidus (Fig. 8). The maximum of temperature on the e_2 (630.7 K)-E_2 (663.1 K) and E_1 (661.8 K)-E_2 (663.1 K) valleys are better visualized on the three-dimension Fig. 8(b).

The thermodynamic parameters of the different phases of the binary and ternary systems are given in Table 3.

5. Conclusions

The Ag-Sb binary system was first reoptimized in order to include our experimental phase diagram data. Using both our experimental phase diagram data of and our enthalpies of mixing of the liquid phase at different temperatures and on different isopleths, the Gibbs energy parameters for the Ag-Au-Sb ternary system were optimized. In general good

agreement was obtained between the calculations and the experiments. However, additional experimental determinations concerning the invariant reaction U_3 are required to confirm the reaction scheme, and the U_2 and U_3 reactions.

Acknowledgments

The authors are grateful to Dr. D. Boa (Laboratoire de Thermodynamique et de Physico-Chimie du Milieu, Université d'Abobo-Adjamé, UFR-SFA, 02 BP 801 Abidjan 02, Côte d'Ivoire) for useful advises on heat of mixing determination of ternary liquid alloys. They are also grateful to Ivorian Government for financial support.

References

1. S. Jin, Developing Lead-Free Solders: A Challenge and Opportunity, *J. Met.*, 1993, **45**, p 13
2. A.T. Dinsdale, A. Kroupa, A. Watson, A. Zemanova, and J. Vrestal, *Release Notes COST 531 Database v 1.1*, Brno, 4th-11th May 2004, 18th-24th September 2004
3. W. Burkhardt and K. Schubert, *Z. Metall*., 1959, **50**, p 442-452
4. E. Zoro, C. Servant, and B. Legendre, Experimental Study of the Phase Diagram of the Ag-Au-Sb Ternary System, *J. Alloys Compd*., 2006, **426**, p 193-199
5. E. Zoro, Contribution à l'étude de nouveaux matériaux de soudure sans plomb: Etude expérimentale et évaluation thermodynamique des systèmes ternaires Ag-Au-Bi/Sb, *Thèse de Doctorat en Sciences*, Université de Paris-Sud, 91405 Orsay Cedex, France, 16 December 2005
6. S. Hassam, J. Agren, M. Gaune-Escard, and J.P. Bros, SGTE Noble Metals Database, *Met. Trans.*, 1990, **21**(7), p 1877-1884
7. J.H. Kim, S.W. Jeong, and H.M. Lee, A Thermodynamic Study of Phase Equilibria in the Au-Sb-Sn Solder System, *J. Electron. Mater.*, 2002, **31**(6), p 557-563
8. C. Oh, J.-H. Shim, B.-J. Lee, and D.N. Lee, A Thermodynamic Study on the Ag-Sb-Sn System, *J. Alloys Compd.*, 1996, **238**, p 155-166
9. H. Okamoto, Phase Diagram Updates Ag-Sb (Silver-Antimony), *J. Phase Equilibria*, 1993, **14**, p 531-532
10. F.N. Rhines, *Phase Diagrams in Metallurgy*. Mc Graw-Hill, New York, 1956, p 201
11. E. Zoro, C. Servant, and B. Legendre, Thermodynamic Re-Assessment of the Ag-Sb System, COST 531 database, version 2.0, Nov 2006
12. O. Redlich and A.T. Kister, Algebraic Representation of Thermodynamic Properties and the Classification of Solutions, *Ind. Eng. Chem.*, 1948, **40**(2), p 345-348
13. Y.M. Muggianu, M. Gambino, and J.P. Bros, Thermodynamic Investigation of Liquid Alloys in Ga-Sb-Bi-Sn System, *J. Chim. Phys.*, 1975, **72**(1), p 83
14. L. Kaufman and H. Berstein, *Computer Calculation of Phase Diagrams*, Academic Press, 1970
15. B. Sundman, B. Jansson, and J.-O. Anderson, The Thermodynamic Databank System, *Calphad*, 1985, **2**(9), p 153-190
16. A.T. Dinsdale, Computer Coupling of Phase Diagrams and Thermochemistry, SGTE Data for Pure Elements, *CALPHAD*, 1991, **15**(4), p 317-425
17. C. Wagner and W. Schottky, Theorie der geordneten Mischphasen, *Z. Phys. Chem. B*, 1930, **11**, p 163-210